DPhG ARCH PHARM
Archiv der Pharmazie

FULL PAPER

Benzoxazole/benzothiazole-derived VEGFR-2 inhibitors: Design, synthesis, molecular docking, and anticancer evaluations

Abdel-Ghany A. El-Helby[1] | Helmy Sakr[1] | Ibrahim H. Eissa[1] |
Ahmed A. Al-Karmalawy[1] | Khaled El-Adl[1,2]

[1]Department of Pharmaceutical Chemistry, Faculty of Pharmacy, Al-Azhar University, Cairo, Egypt

[2]Department of Pharmaceutical Chemistry, Faculty of Pharmacy, Heliopolis University for Sustainable Development, Cairo, Egypt

Correspondence
Khaled El-Adl and Ibrahim H. Eissa, Pharmaceutical Chemistry Department, Faculty of Pharmacy, Al-Azhar University, 1 Al-Mukhayam Al-Daem Street, 6th District, Nassr City, Cairo 00202-2262-5796, Egypt.
Email: eladlkhaled74@yahoo.com; eladlkhaled74@azhar.edu.eg (K. E-A.) and ibrahimeissa@azhar.edu.eg (I. H. E.)

Abstract

A novel series of benzoxazole/benzothiazole derivatives **4a–c**–**11a–e** were designed, synthesized, and evaluated for anticancer activity against HepG2, HCT-116, and MCF-7 cells. HCT-116 was the most sensitive cell line to the influence of the new derivatives. In particular, compound **4c** was found to be the most potent derivative against HepG2, HCT-116, and MCF-7 cells, with IC_{50} values = 9.45 ± 0.8, 5.76 ± 0.4, and 7.36 ± 0.5 μM, respectively. Compounds **4b**, **9f**, and **9c** showed the highest anticancer activities against HepG2 cells with IC_{50} values of 9.97 ± 0.8, 9.99 ± 0.8, and 11.02 ± 1.0 μM, respectively, HCT-116 cells with IC_{50} values of 6.99 ± 0.5, 7.44 ± 0.4, and 8.15 ± 0.8 μM, respectively, and MCF-7 cells with IC_{50} values of 7.89 ± 0.7, 8.24 ± 0.7, and 9.32 ± 0.7 μM, respectively, in comparison with sorafenib as reference drug with IC_{50} values of 9.18 ± 0.6, 5.47 ± 0.3, and 7.26 ± 0.3 μM, respectively. The most active compounds **4a–c**, **9b,c,e,f,h**, and **11c,e** were further evaluated for their VEGFR-2 inhibition. Compounds **4c** and **4b** potently inhibited VEGFR-2 at IC_{50} values of 0.12 ± 0.01 and 0.13 ± 0.02 μM, respectively, which are nearly equipotent to the sorafenib IC_{50} value (0.10 ± 0.02 μM). Furthermore, molecular docking studies were performed for all synthesized compounds to assess their binding pattern and affinity toward the VEGFR-2 active site.

KEYWORDS
anticancer agents, benzothiazole, benzoxazole, molecular docking, VEGFR-2 inhibitors

1 | INTRODUCTION

Extensive studies have been reported on the synthesis of several benzoxazole derivatives as promising anticancer agents[1–5] as potent vascular endothelial growth factor receptor-2 (VEGFR-2) inhibitors,[4,5] for example, compound **I** (Figure 1). Moreover, benzothiazole derivatives have attracted considerable attention as promising and effective anticancer agents[5–7] targeting the VEGFR-2 enzyme.[5,8,9] It was suggested that benzothiazoles act as competitive inhibitors at the ATP-binding site of tyrosine kinases,[5] for example, compound **II** (Figure 1).

The VEGF signaling pathway plays fundamental roles in regulating tumor angiogenesis. VEGF, as a therapeutic target, has been validated in various types of human cancers.[10] VEGFR-2 represents a major target within angiogenesis-related kinases and hence is considered the most important transducer of VEGF-dependent angiogenesis.[11] Thus, inhibition of the VEGF/VEGFR signaling pathway is regarded as an attractive therapeutic target for the inhibition of tumor angiogenesis and subsequent tumor growth.[12–15]

Sorafenib (Nexavar)® is a potent VEGFR-2 inhibitor and has been approved as an antiangiogenic drug.[16–18] Studies on the structure–activity relationships (SAR) and common pharmacophoric
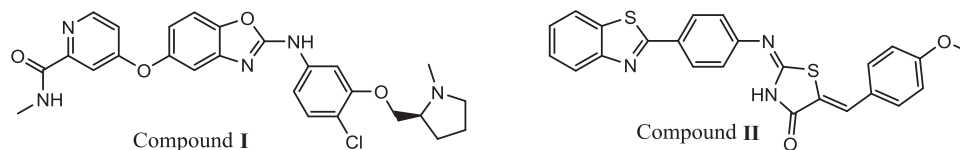
FIGURE 1 Reported benzoxazole and benzothiazole derivatives as VEGFR-2 inhibitors

features shared by sorafenib and various VEGFR-2 inhibitors revealed that most VEGFR-2 inhibitors shared four main features, as shown in Figure 2:[19–21] (a) The core structure of most inhibitors consists of a flat heteroaromatic ring system that contains at least one N atom, which occupies the catalytic adenosine triphosphate (ATP)-binding domain. (b) A central aryl ring (hydrophobic spacer), occupying the linker region between the ATP-binding domain and the DFG domain of the enzyme.[22] (c) A linker containing a functional group acting as a pharmacophore (e.g., amino or urea) that possesses both a H-bond acceptor (HBA) and a donor (HBD) to bind with two crucial residues (Glu883 and Asp1044) in the DFG (Asp–Phe–Gly) motif, an essential tripeptide sequence in the active kinase domain. The NH motifs of the urea or amide moiety usually form one hydrogen bond with Glu883, whereas the C=O motif forms another hydrogen bond with Asp1044. (d) The terminal hydrophobic moiety of the inhibitors occupies the newly created allosteric hydrophobic pocket revealed when the phenylalanine residue of the DFG loop flips out of its lipophilic pocket-defining DFG-out or inactive conformation. Thus, hydrophobic interactions are usually attained in this allosteric binding region.[23] Furthermore, analysis of the X-ray structure of various inhibitors bound to VEGFR-2 confirmed the sufficient space available for various substituents around the terminal heteroaromatic ring.[24–26]

Benzoxazole and benzothiazole nuclei are privileged scaffolds that form the most promising class of heterocycles that are well-tolerated in humans and possess antitumor activity. Moreover, they are the

backbones of many bioactive compounds that show potential activities as VEGFR inhibitors. In addition, several 1,3,4-thiadiazoles,[27,28] thiazolidine-2,4-dione[29] and 6-phenyl-5-cyanothiouracil[30] moieties have been reported to possess anticancer activities.

Depending on the ligand-based drug design, particularly a molecular hybridization approach that involves the coupling of two or more groups with relevant biological properties,[31] molecular hybridization of benzoxazole and/or benzothiazole and other effective antitumor moieties were carried out in an attempt to get new molecules with promising antitumor activities.

In continuation of our efforts to obtain new anticancer agents targeting VEGFR-2, the goal of our work was the synthesis of new agents with the same essential pharmacophoric features of the reported and clinically used VEGFR-2 inhibitors (e.g., sorafenib). The main core of our molecular design rationale comprised bioisosteric modification strategies of VEGFR-2 inhibitors at four different positions (Figure 3).

Our target compounds were designed to have different spacers and different cyclic linkers with HBA–HBD, the main pharmacophoric feature in sorafenib, with the hope to obtain more potent VEGFR-2 inhibitors. First, a bioisosteric approach was adopted in the target benzoxazole and/or benzothiazole to replace the pyridine ring. The second strategy was to use acetamide, 2-sulfanylacetamide and/or 3-sulfanylpropanamide to replace the central aryl ring of the lead structure to increase the flexibility with the aim to increase the VEGFR-2 binding affinity. The third strategy is using cyclic HBA–HBD linkers containing functional groups that possess H-bond acceptors and/or donors, such as 1,3,4-thiadiazoles in compounds **4a–c**, thiazolidine-2,4-dione in compounds **9a–j**, and 6-phenyl-5-cyanothiouracil in compounds **11a–e**. Also, the hydrophobic substituted phenyl tail of the reported ligand was substituted by other groups. Furthermore, the substitution pattern was selected to ensure different electronic and lipophilic environments, which could influence the activity of the target compounds. On the contrary, the linkers were designed in a different way; they constituted a part of the rigid ring structures to study the effect of free-rotated NHCONH of sorafenib and the rigid ring structure linkers on SAR. These modifications were performed to carry out further elaboration of the benzoxazole and/or benzothiazole scaffolds and to explore a valuable SAR. The designed target benzoxazole/benzothiazole derivatives were synthesized and evaluated for their potential VEGFR-2 inhibitory and antitumor activities against three human tumor cell lines: hepatocellular carcinoma (HCC) type (HepG2), breast cancer (Michigan Cancer Foundation-7 [MCF-7]), and human colorectal carcinoma-116 (HCT-116).
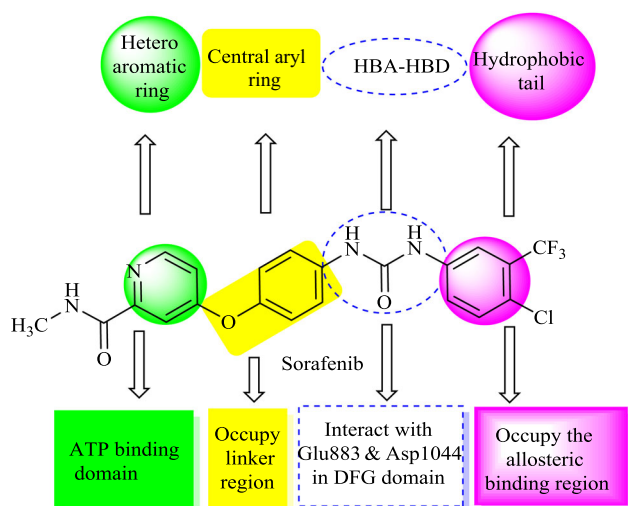
FIGURE 2 The basic structural requirements for sorafenib as reported VEGFR-2 inhibitor. ATP, adenosine triphosphate; HBA, H-bond acceptor; HBD, H-bond donor; VEGFR-2, vascular endothelial growth factor receptor-2
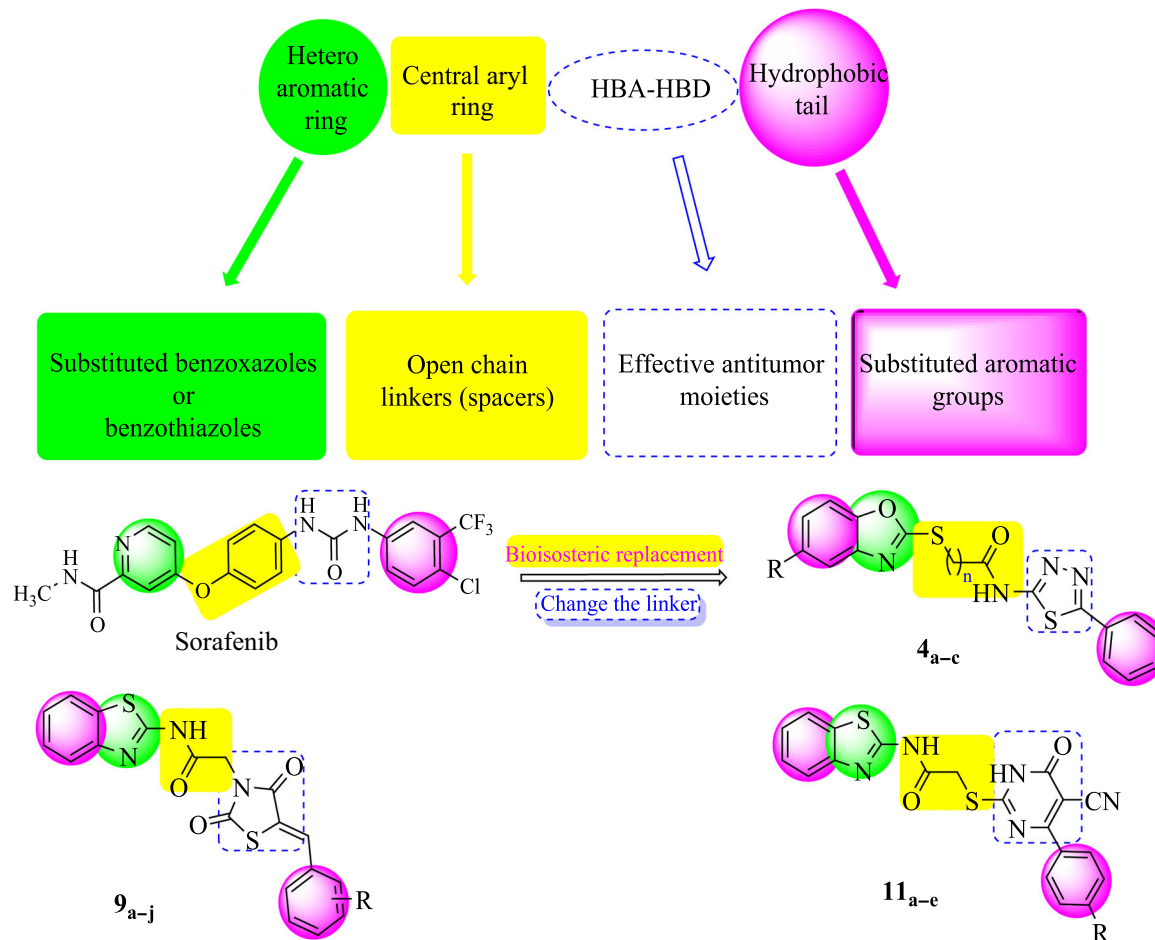
FIGURE 3 Structural similarities and pharmacophoric features of VEGFR-2 inhibitors and the designed compounds. HBA, H-bond acceptor; HBD, H-bond donor; VEGFR-2, vascular endothelial growth factor receptor-2

2 | RESULTS AND DISCUSSION

2.1 | Rationale and structure-based design

Benzoxazole/benzothiazole derivatives impart essential pharmacophoric features to VEGFR-2 inhibitors[32–35] (Figure 3), which include the presence of five-membered hetero rings, oxazole and/or thiazole, fused with a benzene ring, as a hydrophobic portion, forming an aromatic system represented by benzoxazole/benzothiazole rings linked to an (un)substituted hydrophobic distal phenyl ring through different spacers and cyclic linkers (HBA–HBD), which serve as H-bond acceptors through their two Ns with the essential amino acid residue Aspartate1044, also through hydrophobic interaction with its (un)substituted hydrophobic phenyl ring with the hydrophobic pocket lined with the hydrophobic side chains of Alanine864, Valine865, Lysine866, Valine897, Valine914, and Leucine1033. In addition, oxazole and/or other moieties were designed to replace the pyridine moiety of the reference ligand sorafenib. Moreover, the hydrophobic benzoxazole/benzothiazole rings occupied the hydrophobic groove formed by Arginine1025, Histidine1024, Isoleucine1023, Cysteine1022, Leucine1017, Isoleucine890, Histidine889, and Isoleucine886. On the contrary, the cyclic rigid structure

decreased the flexibility of the linkers and the lack of the carbonyl of the urea of sorafenib decreased the binding affinity where it did not form H-bond with the essential amino acid Glutamate883. This may explain the importance of flexible free-rotated linkers.

2.2 | Chemistry

The synthetic strategy for preparation of the target compounds (4–11) is depicted in Schemes 1–3. The synthesis was initiated by cyclocondensation of thiosemicarbazide with benzoic acid to afford 5-phenyl-1,3,4-thiadiazol-2-amine,[36,37] which reacted with the appropriate chloroacyl chloride to afford the corresponding chloroamide (1a,b). On the contrary, 2-amino-4-substituted phenol was reacted with carbon disulphide in the presence of alcoholic potassium hydroxide to provide the corresponding 2-mercapto-benzoxazole derivatives (2a,b), respectively, which were treated with alcoholic potassium hydroxide to afford the corresponding potassium salts (3a,b). The appropriate potassium salt (3a,b) was refluxed with the appropriate chloroamide (1a,b) to afford the corresponding acid amide derivatives (4a–c; Scheme 1). Chloroacetic acid was refluxed with thiourea to afford thiazolidinedione
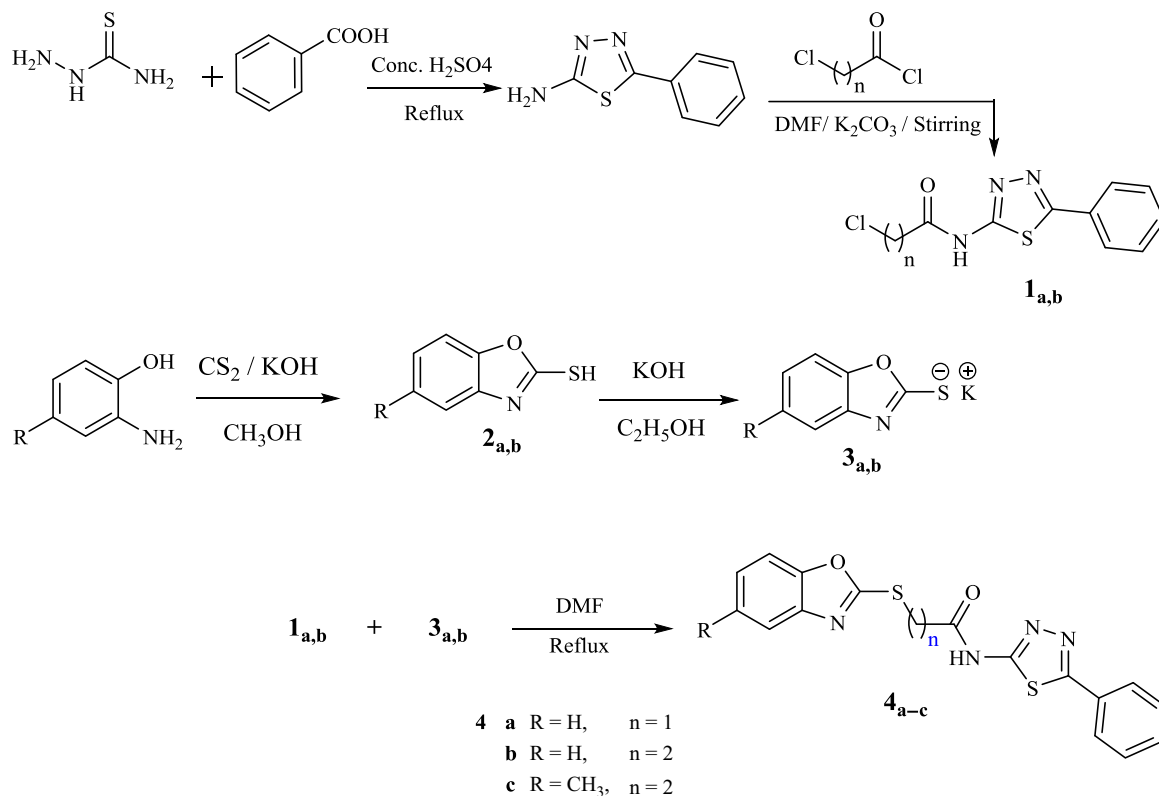
SCHEME 1 Synthetic route for the preparation of the target compounds **4a–c**

(**5**) which underwent reaction with alcoholic potassium hydroxide to produce the corresponding potassium salt (**6**). 2-Aminobenzothiazole was reacted with chloroacetyl chloride to obtain the corresponding chloroamide (**7**), which was refluxed with the obtained potassium salt (**6**) to get the corresponding hybrid benzothiazole thiazolidinedione derivative (**8**). The formed hybrid molecule (**8**) underwent further condensation reaction with the appropriate benzaldehyde, namely, benzaldehyde, 2-chlorobenzaldehyde, 4-chlorobenzaldehyde, 2,6-dichlorobenzaldehyde, 4-fluorobenzaldehyde, 4-methylbenzaldehyde, 2-methoxybenzaldehyde, 4-methoxybenzaldehyde, 4-dimethylaminobenzaldehyde, and/or 3-nitrobenzaldehyde to obtain the corresponding 5-arylidine-2,4-thiazolidinone derivatives by Knoevenagel condensation reaction (**9a–j**), respectively (Scheme 2). Cyclocondensation of ethyl cyanoacetate, thiourea, and the appropriate benzaldehyde, namely, benzaldehyde, 4-fluorobenzaldehyde, 4-methylbenzaldehyde, 4-hydroxybenzaldehyde, and/or 4-methoxybenzaldehyde afforded the corresponding 6-phenyl-5-cyanothiouracil derivatives (**10a–e**) which underwent reaction with the chloroamide (**7**) to produce the corresponding 1,6-dihydropyrimidine derivatives (**11a–e**), respectively (Scheme 3).

2.3 | Docking studies

In the present work, all modeling experiments were performed using Molsoft software. Each experiment used VEGFR-2 downloaded from the Brookhaven Protein Databank (PDB ID 1YWN).[38]

The obtained results indicated that all studied ligands have similar position and orientation inside the putative binding site of VEGFR-2, which reveals a large space bounded by a membrane-binding domain which serves as entry channel for the substrate to the active site (Figure 4). In addition, the affinity of any small molecule can be considered as a unique tool in the field of drug design. There is a relationship between the affinity of organic molecules and the free energy of binding.[39–42] This relationship can contribute to prediction and interpretation of the activity of the organic compounds toward the specific target protein. The obtained results of the free energy of binding (ΔG) explained that most of these compounds had a good binding affinity toward the receptor and the computed values reflected the overall trend (Table 1).

The proposed binding mode of sorafenib revealed an affinity value of −95.36 kcal/mol and four H-bonds. The urea linker formed one H-bond with the key amino acid Glutamate883 (2.13 Å) through its NH group and one H-bond with Aspartate1044 (1.65 Å) through its carbonyl group. The central phenyl ring occupied the hydrophobic pocket formed by Glutamate883, Isoleucine886, Leucine887, Isoleucine1042, Cysteine1043, and Aspartate1044. Moreover, the distal hydrophobic 3-trifluoromethyl-4-chlorophenyl moiety attached to the urea linker occupied the hydrophobic pocket formed by Cysteine1043, Leucine1033, Valine897, Valine914, Alanine864, Valine865, and Lysine866. Furthermore, the *N*-methylpicolinamide moiety occupied the hydrophobic groove formed by Arginine1025, Histidine1024, Isoleucine1023, Cysteine1022, Leucine1017,
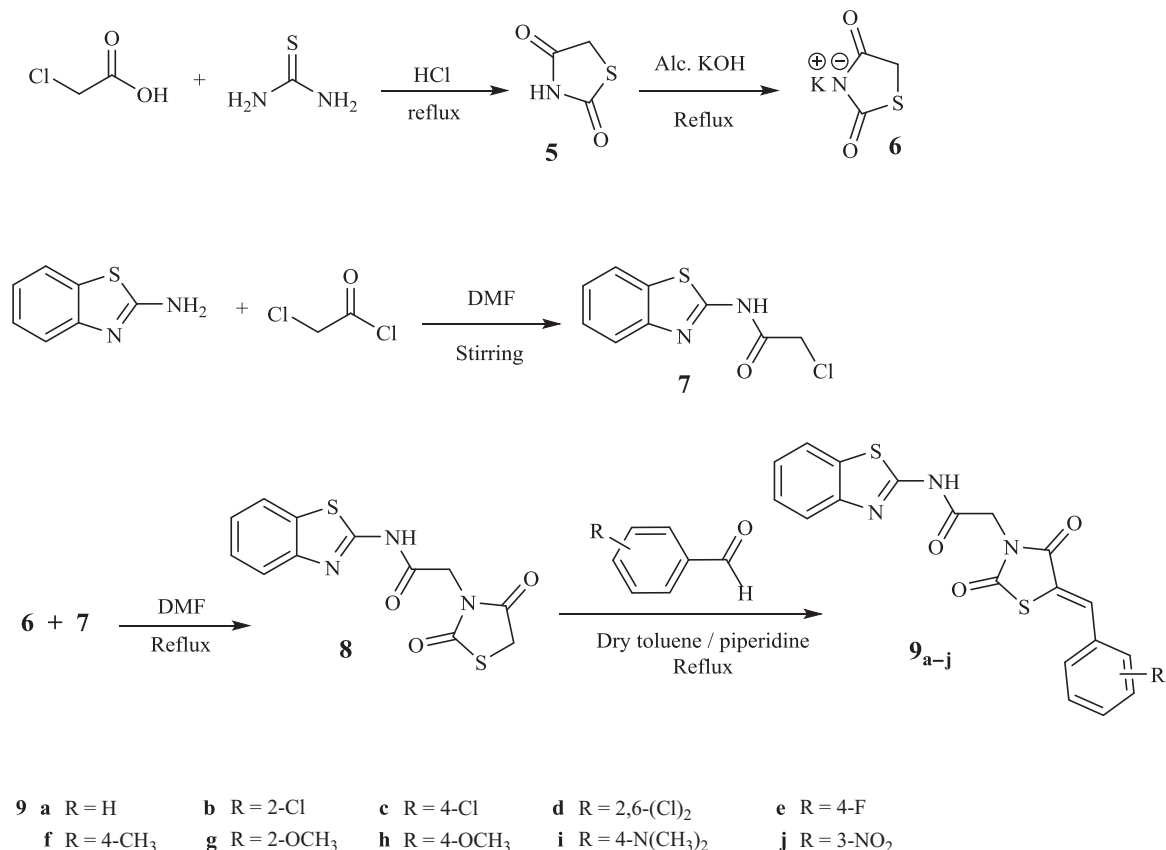
SCHEME 2 Synthetic route for the preparation of the target compounds **8–j** and **9a–j**

9 a R = H	**b** R = 2-Cl	**c** R = 4-Cl	**d** R = 2,6-(Cl)$_2$	**e** R = 4-F
f R = 4-CH$_3$	**g** R = 2-OCH$_3$	**h** R = 4-OCH$_3$	**i** R = 4-N(CH$_3$)$_2$	**j** R = 3-NO$_2$

Isoleucine890, Histidine889, and Isoleucine886, whereas its carbonyl was stabilized by the formation of two H-bonds with Arginine1025 (1.90 and 2.12 Å; Figure 5). The urea linker played an important role in the binding affinity towards VEGFR-2 enzyme, where it was responsible for the higher binding affinity of sorafenib. This finding encourages us to use different cyclic linkers resembling urea of sorafenib, hoping to obtain potent VEGFR-2 inhibitors.

As planned, the proposed binding mode of compound **4c** is virtually the same as that of sorafenib which revealed affinity nearly the same as that of sorafenib with a value of −94.71 kcal/mol and four H-bonds. The 1,3,4-thiadiazole linker was stabilized by the formation of three H-bonds with Aspartate1044 (1.43, 2.30, and 2.88 Å). The SCH$_2$CH$_2$CONH spacer formed one H-bond with Aspartate1044 (2.58 Å) through its carbonyl group. It also occupied

11 a R = H	**b** R = F	**c** R = CH$_3$
d R = OH	**e** R = OCH$_3$	
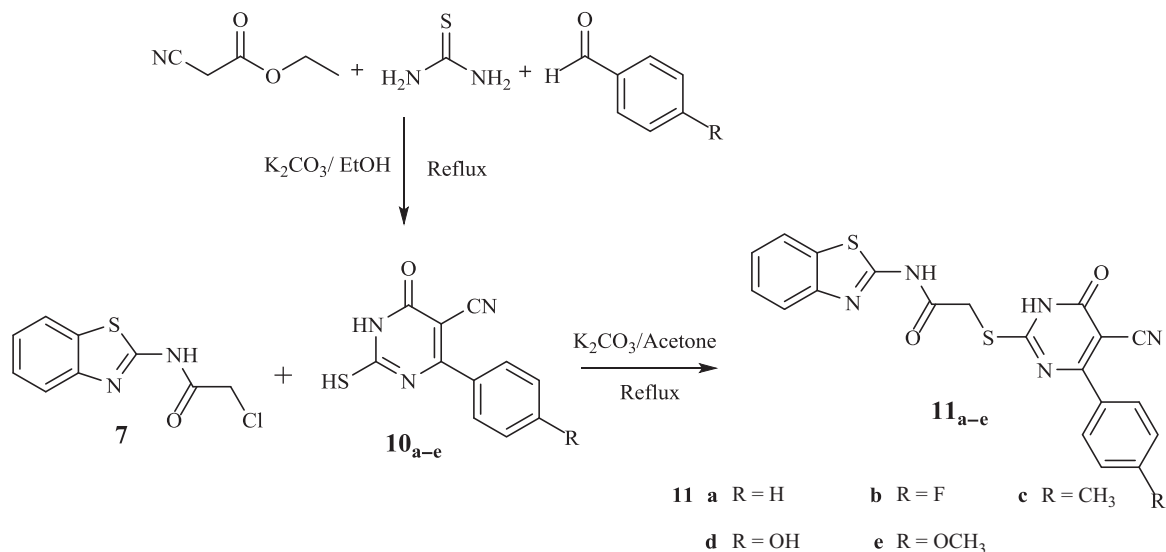
SCHEME 3 Synthetic route for the preparation of the target compounds **11a–e**
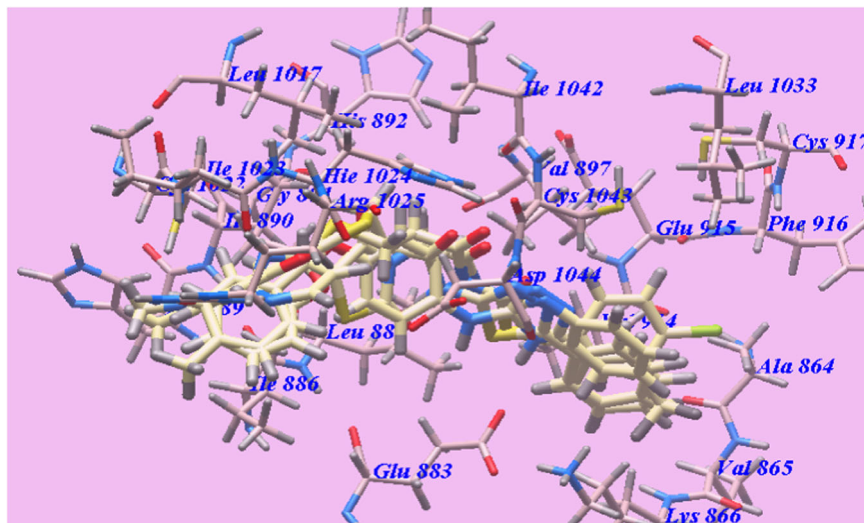
FIGURE 4 Superimposition of some docked compounds inside the binding pocket of 1YWN

the hydrophobic pocket formed by Glutamate883, Isoleucine886, Leucine887, Leucine1017, Histidine1024, Isoleucine1042, Cysteine1043, and Aspartate1044. The distal phenyl moiety occupied the hydrophobic pocket formed by Leucine1033, Valine897, Valine914, Glutamate915, Phenylalanine916, Cysteine917, Alanine864, Valine865, Lysine866, and Glutamate883. Furthermore, the benzoxazole moiety occupied the hydrophobic groove formed by Arginine1025, Histidine1024, Isoleucine1023, Cysteine1022, Isoleucine890, Histidine889, and Isoleucine886 (Figure 6). These interactions of compound **4c** may explain the highest anticancer activity.

The proposed binding mode of compound **4b** is virtually the same as that of **4c** which revealed an affinity value of −92.39 kcal/mol and four H-bonds. The 1,3,4-thiadiazole linker was stabilized by the formation of three H-bonds with Aspartate1044 (1.57, 2.68, and 2.79 Å). The SCH_2CH_2CONH spacer formed one H-bond with Aspartate1044 (1.87 Å) through its carbonyl group. It also occupied the hydrophobic pocket formed by Glutamate883, Isoleucine886, Leucine887, Leucine1017, Histidine1024, Isoleucine1042, Cysteine1043, and Aspartate1044. The distal phenyl moiety occupied the hydrophobic pocket formed by Leucine1033, Valine897, Valine914, Glutamate915, Phenylalanine916, Cysteine917,

Alanine864, Valine865, Lysine866, and Glutamate883. Furthermore, the benzoxazole moiety occupied the hydrophobic groove formed by Arginine1025, Histidine1024, Isoleucine1023, Cysteine1022, Isoleucine890, Histidine889, and Isoleucine886 (Figure 7). These interactions of compound **4b** may explain the higher anticancer activity.

From the obtained docking results (Table 1), we concluded that free-rotated urea linker is essential for higher affinity towards VEGFR-2 enzyme than the cyclic linkers. The longer SCH_2CH_2CONH spacer showed higher binding affinities than the SCH_2CONH one. The 1,3,4-thiadiazoles exhibited higher affinities than thiazolidine-2,4-dione and 1,6-dihydropyrimidine, respectively. Also, lipophilicity played an important role in their VEGFR-2 inhibitory activities which may be due to higher hydrophobic interactions.
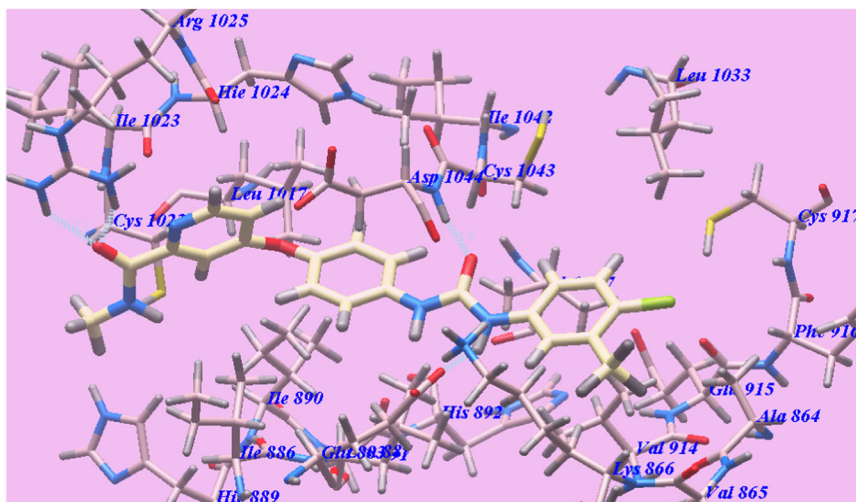
2.4 | In vitro cytotoxic activity

Antiproliferative activity of the newly synthesized benzoxazole/benzothiazole derivatives **4a–c–11a–e** was examined against three human tumor cell lines namely, HepG2, MCF-7, and HCT-116 using 3-(4,5-dimethylthiazol-2-yl)-2,5-diphenyltetrazolium bromide (MTT) colorimetric assay as described by Mosmann.[43–45] Sorafenib was included in the experiments as a reference cytotoxic drug. The results were expressed as growth inhibitory concentration (IC_{50}) values, which represent the compound concentrations required to produce a 50% inhibition of cell growth after 72 hr of incubation calculated from the concentration–inhibition response curve and summarized in Table 2. From the obtained results, it was explicated that most of the prepared compounds displayed an excellent to modest growth inhibitory activity against the tested cancer cell lines. Investigations of the cytotoxic activity against HCT-116 and MCF-7 indicated that they were more sensitive cell lines to the influence of the new derivatives, respectively. In particular, compound **4c** was found to be the most potent derivative overall the tested compounds against HepG2, HCT-116, and MCF-7 cancer cell lines with $IC_{50} = 9.45 \pm 0.8$, 5.76 ± 0.4, and 7.36 ± 0.5 μM, respectively. It has nearly the same activity as sorafenib against the three cell lines ($IC_{50} = 9.18 \pm 0.6$, 5.47 ± 0.3, and

**TABLE 1** The calculated ΔG (free energy of binding) and binding affinities for the ligands (ΔG in kcal/mol)

| Compound	ΔG (kcal/mol)	Compound	ΔG (kcal/mol)
4a	−82.78	9g	−77.30
4b	−92.39	9h	−84.22
4c	−94.71	9i	−80.98
8	−71.37	9j	−74.32
9a	−74.07	11a	−74.89
9b	−82.90	11b	−80.56
9c	−86.03	11c	−85.52
9d	−82.12	11d	−79.89
9e	−85.83	11e	−82.59
9f	−89.58	Sorafenib	−95.36

FIGURE 5 Predicted binding mode for sorafenib with 1WYN. H-bonded atoms are indicated by dotted lines

FIGURE 6 Predicted binding mode for **4c** with 1WYN
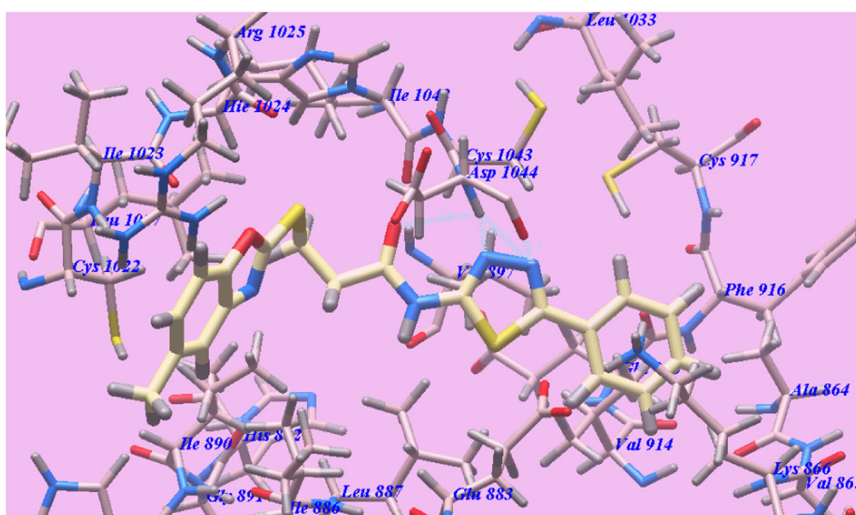
FIGURE 7 Predicted binding mode for **4b** with 1WYN
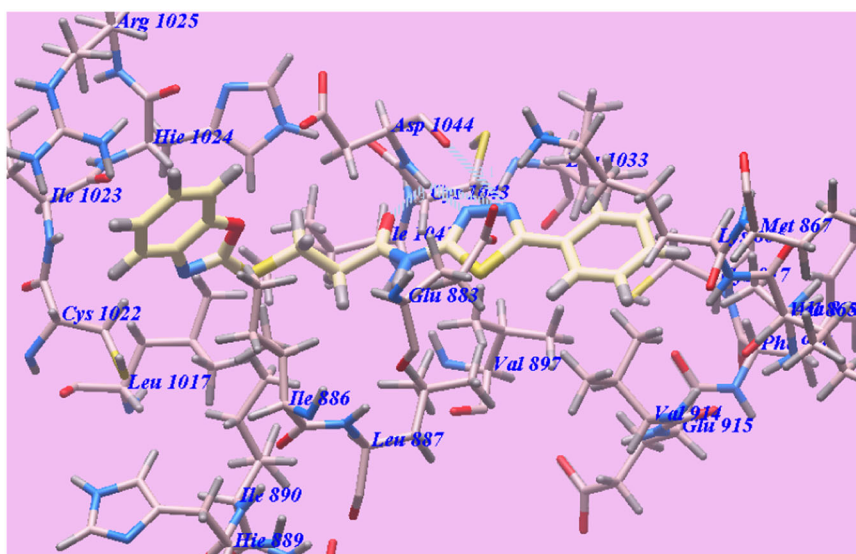
TABLE 2 In vitro cytotoxic activities of the newly synthesized compounds against HepG2, MCF-7, and HCT-116 cell lines and VEGFR-2 kinase assay

	IC_{50} (µM)[a]					IC_{50} (µM)[a]			
Compd	HepG2	HCT-116	MCF-7	VEGFR-2	Compd	HepG2	HCT-116	MCF-7	VEGFR-2
4a	15.88 ± 1.2	12.45 ± 1.2	12.65 ± 1.1	0.22 ± 0.02	9g	24.74 ± 2.4	24.77 ± 2.4	24.99 ± 2.3	NT
4b	9.97 ± 0.8	6.99 ± 0.5	7.89 ± 0.7	0.13 ± 0.02	9h	14.06 ± 1.1	11.16 ± 1.1	12.17 ± 1.2	0.21 ± 0.02
4c	9.45 ± 0.8	5.76 ± 0.4	7.36 ± 0.5	0.12 ± 0.01	9i	23.24 ± 1.9	22.11 ± 2.0	22.15 ± 2.2	NT
8	34.55 ± 3.1	32.77 ± 3.2	34.13 ± 3.2	NT	9j	25.88 ± 2.3	24.87 ± 2.3	24.44 ± 2.3	NT
9a	25.65 ± 2.3	25.59 ± 2.3	26.08 ± 2.3	NT	11a	25.15 ± 2.1	22.66 ± 2.2	24.54 ± 2.3	NT
9b	16.32 ± 1.4	15.43 ± 1.4	14.55 ± 1.4	0.25 ± 0.02	11b	23.78 ± 1.9	23.33 ± 2.0	22.44 ± 2.1	NT
9c	11.02 ± 1.0	8.15 ± 0.8	9.32 ± 0.7	0.16 ± 0.02	11c	12.12 ± 1.1	12.14 ± 1.1	10.34 ± 1.0	0.19 ± 0.02
9d	19.09 ± 1.7	21.12 ± 1.7	17.23 ± 1.8	NT	11d	23.97 ± 2.1	23.89 ± 2.2	23.65 ± 2.3	NT
9e	11.67 ± 0.9	8.88 ± 0.8	9.94 ± 0.6	0.19 ± 0.01	11e	17.99 ± 1.6	16.22 ± 1.4	14.97 ± 1.3	0.30 ± 0.03
9f	9.99 ± 0.8	7.44 ± 0.4	8.24 ± 0.7	0.15 ± 0.02	Sorafenib	9.18 ± 0.6	5.47 ± 0.3	7.26 ± 0.3	0.10 ± 0.02

Abbreviations: HCT-116, human colorectal carcinoma-116; HepG2, hepatocellular carcinoma (HCC) type; MCF-7, Michigan Cancer Foundation-7; NT, compounds not tested for their VEGFR-2 inhibitory activity; SD, standard deviation; VEGFR-2, vascular endothelial growth factor receptor-2.

[a]IC_{50} values are the mean ± SD of three separate experiments.

7.26 ± 0.3 µM, respectively). With respect to the HepG2 hepatocellular carcinoma cell line, compounds **4b**, **9f**, **9c**, **9e**, and **11c** displayed the highest anticancer activities with (IC_{50} = 9.97 ± 0.8, 9.99 ± 0.8, 11.02 ± 1.0, 11.67 ± 0.9, and 12.12 ± 1.1 µM, respectively). Compounds **4a**, **9b,d,h**, and **11e**, with IC_{50} ranging from 14.06 ± 1.1 to 19.09 ± 1.7 µM, displayed good cytotoxicity. Compounds **9a,g,i,j** and **11a,b,d**, with IC_{50} ranging from 23.24 ± 1.9 to 25.88 ± 2.3 µM exhibited moderate cytotoxicity; whereas compound **8** with IC_{50} = 34.55 ± 3.1 µM exhibited the lowest cytotoxicity.

Cytotoxicity evaluation against colorectal carcinoma (HCT-116) cell line discovered that compounds **4b**, **9f**, **9c**, **9e**, **9h**, **11c**, and **4a** displayed the highest anticancer activities with IC_{50} = 6.99 ± 0.5, 7.44 ± 0.4, 8.15 ± 0.8, 8.88 ± 0.8, 11.16 ± 1.1, 12.14 ± 1.1, and 12.45 ± 1.2 µM, respectively. Compounds **9b,d** and **11e**, with IC_{50} ranging from 15.43 ± 1.4 to 21.12 ± 1.7 µM, displayed good cytotoxicity. Compounds **9a,g,i,j** and **11a,b,d**, with IC_{50} ranging from 22.11 ± 2.0 to 25.59 ± 2.3 µM, exhibited moderate cytotoxicity; whereas compound **8** with IC_{50} = 32.77 ± 3.2 µM exhibited the lowest cytotoxicity.

Cytotoxicity evaluation against MCF-7 cell line revealed that compounds **4b**, **9f**, **9c**, **9e**, and **11c** displayed the highest anticancer activities (with IC_{50} = 7.89 ± 0.7, 8.24 ± 0.7, 9.32 ± 0.7, 9.94 ± 0.6, and 10.34 ± 1.0 µM, respectively). Compounds **4a**, **9b,d,h**, and **11e** (with IC_{50} ranging from 12.17 ± 1.2 to 14.97 ± 1.3 µM) displayed good cytotoxicity. Compounds **9a,g,b,i,j** and **11a,b,d** (with IC_{50} ranging from 22.15 ± 2.2 to 26.08 ± 2.3 µM) exhibited moderate cytotoxicity; whereas compound **8** with IC_{50} = 34.13 ± 3.2 µM exhibited the lowest cytotoxicity.

2.5 | In vitro VEGFR-2 kinase assay

The most active antiproliferative derivatives **4a–c**, **9b,c,e,f,h**, and **11c,e** were selected to evaluate their inhibitory activities against

VEGFR-2 by using an antiphosphotyrosine antibody with the Alpha Screen system (PerkinElmer). The results were reported as a 50% inhibition concentration value (IC_{50}) calculated from the concentration–inhibition response curve and summarized in Table 2. Sorafenib was used as a positive control in this assay. The tested compounds displayed high to good inhibitory activity with IC_{50} values ranging from 0.12 ± 0.01 to 0.30 ± 0.03 µM. Among them, compounds **4c** and **4b** potently inhibited VEGFR-2 at IC_{50} values of 0.12 ± 0.01 and 0.13 ± 0.02 µM, respectively, which are nearly equipotent as sorafenib IC_{50} value (0.10 ± 0.02 µM). Also, compounds **4b**, **9f**, **9c**, **9e**, and **11c** possessed good VEGFR-2 inhibition with IC_{50} values of 0.13 ± 0.02, 0.15 ± 0.02, 0.16 ± 0.02, 0.19 ± 0.01, and 0.19 ± 0.02 µM, respectively; whereas compounds **9h**, **4a**, **9b**, and **11c** possessed moderate VEGFR-2 inhibition with IC_{50} values of 0.21 ± 0.02, 0.22 ± 0.02, 0.25 ± 0.02, and 0.30 ± 0.03 µM, respectively.

2.6 | Structure–activity relationship (SAR)

The preliminary SAR study has focused on the effect of replacement of the free-rotated urea linker of sorafenib with different cyclic linkers which interact as H-bond acceptors through their N-atoms as in compounds **4a–c** or their carbonyl groups as in compounds **9a–j** or as H-bond donors through their NH atoms and as H-bond acceptors through their carbonyl groups as in compounds **11a–c**. These cyclic linkers interact with the side-chain carboxylate of the essential amino acid residue Aspartate1044. Also, hydrophobic interactions occur through the attached (un)substituted hydrophobic moieties. The effect of replacement of pyridine moiety of sorafenib by the benzoxazole/benzothiazole scaffolds of the synthesized compounds on the antitumor activities also was noticed. The benzoxazole/benzothiazole scaffolds occupied the same hydrophobic pocket as occupied by the pyridine moiety of the standard ligand. On the contrary, different hydrophobic groups were introduced instead of

the phenyl moiety of the reference ligand. Moreover, different substitutions were introduced to the phenyl group with different lipophilicity and electronic nature to study their effect in the anticancer activity. The data obtained revealed that the tested compounds displayed different levels of anticancer activity and possessed a distinctive pattern of selectivity against the HCT-116 and MCF-7 cell lines, respectively. Generally, the spacers, linkers (HBA–HBD), lipophilicity, and electronic nature exhibited an important role in anticancer activity. The 1,3,4-thiadiazoles linkers of compounds 4a–c were found to be responsible for the higher anticancer activity than that of thiazolidine-2,4-dione as in compounds 9a–j and 6-phenyl-5-cyanothiouracil as in compounds 11a–e, respectively. The SCH$_2$CH$_2$CONH spacers as in compounds 4b,c resulted in higher activities than the SCH$_2$CONH one as in 4a or 11a–e and CH$_2$CONH, respectively. The spacer SCH$_2$CONH as in compounds 4a–c showed higher activities than the retroarrangement HNCOCH$_2$S as in compounds 11a–e. From the structure of the synthesized derivatives and the data shown in Table 2 we can divide these tested compounds into three groups. The first group is compounds 4a–c, where the 5-methylbenzoxazole derivatives for example compound 4c showed higher activities than the unsubstituted ones, for example, compounds 4b and 4a, respectively. In the second group 9a–j, the distal phenyl group played an important role in an activity where, the substituted phenyl group as in compounds 9b–j exhibited higher activities than the unsubstituted one 9a. The 4-substituted phenyl group, for example, 9c and 9h exhibited higher activities than the 2-substituted, for example, 9b and 9g and/or 3-substituted ones as 9j, respectively. The lipophilic electron-donating methyl group at position 4 as in compounds 9f displayed higher anticancer activity than the electron-withdrawing Cl group as in compound 9e and F group as in 9c, respectively. The more lipophilic substituents at position 4 as CH$_3$, Cl, and F as in compounds 9a–c exhibited higher activities than the lower lipophilic substituents as methoxy and dimethylamino groups as in 9h and 9i, respectively. The monosubstituted derivatives as in compounds 9c and 9b showed higher activities than the disubstituted one as in compound 9d. In the third group 11a–e, the substituted distal phenyl group as in compounds 11b–e exhibited higher activities than the unsubstituted one 11a. The lipophilic electron-donating methyl and methoxy groups as in compounds 11c and 11e exhibited higher anticancer activities than the electron-withdrawing F group as in compound 11b, respectively. The lipophilic electron-donating methyl and methoxy groups as in compounds 11c and 11e exhibited higher anticancer activities than the hydrophilic electron-donating OH group as in compound 11d, respectively.

3 | CONCLUSION

The molecular design was performed to investigate the binding mode of the proposed compounds with VEGFR-2 receptor. The data obtained from the docking studies were fitted with that obtained from the biological screening. All the tested compounds showed variable anticancer activities. Novel series of benzoxazole/benzothiazole derivatives 4a–c–11a–e were designed, synthesized and evaluated for their anticancer activity against three human tumor cell lines HepG2, HCT-116, and MCF-7 targeting VEGFR-2 enzyme. HCT-116 and MCF-7 were the most sensitive cell lines to the influence of the new derivatives. In particular, compound 4c was found to be the most potent derivative against HepG2, HCT-116, and MCF-7 with IC$_{50}$ = 9.45 ± 0.8, 5.76 ± 0.4, and 7.36 ± 0.5 μM, respectively. Compounds 4b, 9f, and 9c showed the highest anticancer activities against HepG2 with IC$_{50}$ of 9.97 ± 0.8, 9.99 ± 0.8, and 11.02 ± 1.0 μM, respectively; HCT-116 with IC$_{50}$ of 6.99 ± 0.5, 7.44 ± 0.4, and 8.15 ± 0.8 μM, respectively; and MCF-7 with IC$_{50}$ of 7.89 ± 0.7, 8.24 ± 0.7, and 9.32 ± 0.7 μM, respectively, in comparison with sorafenib as a reference drug with IC$_{50}$ of 9.18 ± 0.6, 5.47 ± 0.3, and 7.26 ± 0.3 μM, respectively. The most active compounds 4a–c, 9b,c,e,f,h, and 11c,e were further evaluated for their VEGFR-2 inhibition. Compounds 4c and 4b potently inhibited VEGFR-2 at IC$_{50}$ values of 0.12 ± 0.01 and 0.13 ± 0.02 μM, respectively, which are nearly equipotent as sorafenib IC$_{50}$ value (0.10 ± 0.02 μM). The obtained results showed that the most active compounds could be useful as a template for future design, optimization, adaptation, and investigation to produce more potent and selective VEGFR-2 inhibitors with higher anticancer analogs.

4 | EXPERIMENTAL

4.1 | Chemistry

4.1.1 | General

All melting points were carried out by open capillary method on a Gallenkamp melting point apparatus at Faculty of Pharmacy of Al-Azhar University and were uncorrected. The infrared spectra were recorded on Pye Unicam SP 1000 IR (infrared) spectrophotometer at Pharmaceutical Analytical Unit, Faculty of Pharmacy, Al-Azhar University using potassium bromide disc technique. Proton magnetic resonance ^{1}H-NMR spectra were recorded on a Bruker 400 MHZ-NMR spectrometer at Faculty of Sciences, Cairo University, Cairo, Egypt. ^{13}C-NMR spectra were recorded on an Agilent 400 MHZ-NMR spectrometer at Chemical Laboratory, Ministry of Defense, Cairo. TMS (tetramethylsilane) was used as internal standard and chemical shifts were measured in δ scale (ppm). The mass spectra were carried out on Direct Probe Controller Inlet part to Single Quadropole mass analyzer in Thermo Scientific GCMS model ISQ LT using Thermo X-Calibur software at the Regional Center for Mycology and Biotechnology, Al-Azhar University. Elemental analyses (C, H, and N) were performed on a CHN analyzer at Regional Center for Mycology and Biotechnology, Al-Azhar University. All compounds were within ±0.4 of the theoretical values. The reactions were monitored by thin-layer chromatography (TLC) using TLC sheets precoated with UV fluorescent silica gel Merck 60 F254 plates and were visualized using UV lamp and different solvents as mobile phases.

2-Chloro-N-(5-phenyl-1,3,4-thiadiazol-2-yl)acetamide (**1a**) 3-chloro-N-(5-phenyl-1,3,4-thiadiazol-2-yl)propanamide (**1b**), 2-mercaptobenzoxazole (**2a**), 2-mercapto-5-methylbenzoxazole (**2b**), and their corresponding potassium salts (**3a,b**), thiazolidine-2,4-dione (**5**), its potassium salt (**6**), N-(benzothiazol-2-yl)-2-chloroacetamide (**7**), and 2-mercapto-6-oxo-4-(4-(un)substituted phenyl)-1,6-dihydropyrimidine-5-carbonitrile (**10**) were obtained according to the reported procedures.[35,36]

The InChI codes of the investigated compounds together with some biological activity data are provided as Supporting Information.

4.1.2 | General method for the synthesis of 2-(benzoxazol-2-ylthio)-N-(5-phenyl-1,3,4-thiadizol-2-yl)acetamide (4a) and N-(5-phenyl-1,3,4-thiadizol-2-yl)-3-[5-(un)substituted benzoxazol-2-ylthio]-propanamides (4b,c)

To a mixture of the potassium salts **3a** and/or **3b** (0.002 mol) in dry DMF (50 ml), the appropriate chloroamide derivatives (**1a,b**; 0.002 mol) were added. The reaction mixture was heated using a water bath for 12 hr. After cooling to room temperature, reaction mixture was poured onto crushed ice. The precipitated solids were collected by filtration, dried, and crystallized from ethanol to give the target compounds **4a–c**.

2-(Benzoxazol-2-ylthio)-N-(5-phenyl-1,3,4-thiadiazol-2-yl)acetamide (4a)

Yield, 81%; m.p. 176–178°C; IR$_{\nu max}$ (cm^{-1}): 3,171 (NH), 3,037 (CH aromatic), 2,915 (CH aliphatic), and 1,690 (C=O); ^{1}H-NMR (400 MHz, dimethyl sulfoxide [DMSO]-d_6): 4.51 (s, 2H, CH$_2$), 7.28 (dd, 1H, J = 8, 7 Hz; Ar-H, H-6 of benzoxazole), 7.49 (dd, 1H, J = 8.8, 7 Hz; Ar-H, H-5 of benzoxazole), 7.55 (dd, 1H, J = 8.6, 8.6 Hz; Ar-H, H-4 of phenyl), 7.60 (dd, 2H, J = 8.6, 9.6 Hz; Ar-H, H-3 and H-5 of phenyl), 7.89 (d, 1H, J = 8.8 Hz; Ar-H, H-4 of benzoxazole), 7.91 (d, 1H, J = 8 Hz; Ar-H, H-7 of benzoxazole), 7.95 (d, 2H, J = 9.6 Hz; Ar-H, H-2 and H-6 of phenyl), and 13.11 (s, 1H, NH; D$_2$O exchangeable); MS (m/z): 368 (M$^+$, 100%, base peak), 295 (29.10%), 204 (7.50%), 121 (14.78%), and 77 (15.65%); Anal. calcd. for C$_{17}$H$_{12}$N$_4$O$_2$S$_2$ (m.w. 368.43): C, 55.42; H, 3.28; N, 15.21; S, 17.40. Found: C, 55.71; H, 3.25; N, 15.11; S, 17.48.

3-(Benzoxazol-2-ylthio)-N-(5-phenyl-1,3,4-thiadiazol-2-yl)propanamide (4b)

Yield, 76%; m.p. 215–217°C; IR$_{\nu max}$ (cm^{-1}): 3,168 (NH), 3,038 (CH aromatic), 2,905 (CH aliphatic), and 1,688 (C=O); ^{1}H-NMR (400 MHz, DMSO-d_6): 3.10 (t, 2H, J = 6.8 Hz, –CH$_2$CO), 4.51 (t, 2H, J = 6.8 Hz, –SCH$_2$), 7.30 (dd, 1H, J = 7.6, 7.2 Hz; Ar-H, H-6 of benzoxazole), 7.37 (dd, 1H, J = 7.6, 8 Hz; Ar-H, H-5 of benzoxazole), 7.52 (dd, 1H, J = 7.6, 7.6 Hz; Ar-H, H-4 of phenyl), 7.56 (dd, 2H, J = 6.6, 7.6 Hz; Ar-H, H-3 and H-5 of phenyl), 7.65 (d, 1H, J = 8 Hz; Ar-H, H-4 of benzoxazole), 7.93 (d, 1H, J = 7.2 Hz; Ar-H, H-7 of benzoxazole), 7.95 (d, 2H, J = 6.6 Hz; Ar-H, H-2 and H-6 of phenyl), and 12.82 (s, 1H, NH; D$_2$O exchangeable); Anal. calcd. for C$_{18}$H$_{14}$N$_4$O$_2$S$_2$ (m.w. 382.46): C,

56.53; H, 3.69; N, 14.65; S, 16.77. Found: C, 56.45; H, 3.63; N, 15.02; S, 16.74.

3-((5-Methylbenzoxazol-2-yl)thio)-N-(5-phenyl-1,3,4-thiadiazol-2-yl)-propanamide (4c)

Yield, 79%; m.p. 273–275°C; IR$_{\nu max}$ (cm^{-1}): 3,164 (NH), 3,090 (CH aromatic), 2,908 (CH aliphatic), and 1,689 (C=O); ^{1}H-NMR (400 MHz, DMSO-d_6): 2.36 (s, 3H, CH$_3$), 3.07 (t, J = 6.8 Hz; 2H, –CH$_2$CO), 4.53 (t, J = 6.8 Hz; 2H, –SCH$_2$), 6.48 (d, 1H, J = 8.4 Hz; Ar-H, H-6 of benzoxazole), 6.55 (dd, 1H, J = 8, 8 Hz; Ar-H, H-4 of phenyl), 7.11 (dd, 2H, J = 7.6, 8 Hz; Ar-H, H-3 and H-5 of phenyl), 7.37 (s, 1H; Ar-H, H-4 of benzoxazole), 7.53 (d, 1H, J = 8.4 Hz; Ar-H, H-7 of benzoxazole), 7.94 (d, 2H, J = 7.6 Hz; Ar-H, H-2 and H-6 of phenyl), and 12.90 (s, 1H, NH; D$_2$O exchangeable); Anal. calcd. for C$_{19}$H$_{16}$N$_4$O$_2$S$_2$ (m.w. 396.48): C, 57.56; H, 4.07; N, 14.13; S, 16.17. Found: C, 57.12; H, 4.32; N, 14.01; S, 16.46.

4.1.3 | Synthesis of N-(benzothiazol-2-yl)-2-(2,4-dioxothiazolidin-3-yl)acetamide (8)

A mixture of the potassium salt of thiazolidin-2,4-dione (**6**; 1.55 g, 0.01 mol) and N-(benzothiazol-2-yl)-2-chloroacetamide (**7**; 2.26 g, 0.01 mol) in dry DMF (20 ml) was heated on a water bath for 20 hr. After cooling, the reaction mixture was poured on crushed ice. The formed precipitate was filtered, dried, and crystallized from ethanol affording the desired product (**8**; 2.63 g) as a beige solid.

Yield, 85%; m.p. 171–173°C; IR$_{\nu max}$ (cm^{-1}): 3,328 (NH), 3,090 (CH aromatic), 2,991 (CH aliphatic), and 1,674 (C=O); ^{1}H-NMR (400 MHz, DMSO-d_6): 2.65 (s, 2H, CH$_2$S), 4.30 (s, 2H, CH$_2$N), 7.26 (dd, 1H, J = 8, 7 Hz; Ar-H, H-5 of benzothiazole), 7.42 (dd, 1H, J = 8, 7.6 Hz; Ar-H, H-6 of benzothiazole), 7.70 (d, 1H, J = 7.6 Hz; Ar-H, H-7 of benzothiazole), 7.91 (d, 1H, J = 7 Hz; Ar-H, H-4 of benzothiazole), and 12.30 (s, 1H, NH; D$_2$O exchangeable); MS (m/z): 307 (M$^+$, 4.03%), 177 (38.30%), 150 (100%, base peak), 135 (27.49%), and 69 (30.44%); Anal. calcd. for C$_{12}$H$_9$N$_3$O$_3$S$_2$ (307.34): C, 46.90; H, 2.95; N, 13.67; S, 20.86. Found: C, 46.47; H, 3.18; N, 13.37; S, 21.27.

4.1.4 | General method for the synthesis of N-(benzothiazol-2-yl)-2-[5-(un)substituted benzylidene-2,4-dioxothiazolidin-3-yl]acetamide (9a–j)

A mixture of N-(benzothiazol-2-yl)-2-(2,4-dioxothiazolidin-3-yl)acetamide **8** (0.307 g, 0.001 mol) and the appropriate benzaldehyde (0.001 mol) namely benzaldehyde, 2-chlorobenzaldehyde, 4-chlorobenzaldehyde, 2,6-dichlorobenzaldehyde, 4-fluorobenzaldehyde, 4-methylbenzaldehyde, 2-methoxybenzaldehyde, 4-methoxybenzaldehyde, 4-N,N-dimethylaminobenzaldehyde, and/or 3-nitrobenzaldehyde in the presence of catalytic quantity of piperidine was refluxed in dry toluene for 8 hr. The reaction mixture was cooled to 25°C to obtain a solid product. The product was crystallized from ethanol to give the corresponding target compounds **9a–j**, respectively.

N-(Benzothiazol-2-yl)-2-(5-benzylidene-2,4-dioxothiazolidin-3-yl)-acetamide (9a)

Yield, 90%; m.p. 232–233°C; IR$_{\nu max}$ (cm^{-1}): 3,199 (NH), 3,080 (CH aromatic), 2,999 (CH aliphatic), and 1,698 (C=O); ^{1}H-NMR (400 MHz, DMSO-d_6): 4.71 (s, 2H, CH$_2$), 7.31 (dd, 1H, J = 8, 8 Hz; Ar-H, H-4 of phenyl), 7.44 (dd, 1H, J = 7.6, 7.6 Hz; Ar-H, H-5 of benzothiazole), 7.51 (dd, 1H, J = 7.6, 8 Hz; Ar-H, H-6 of benzothiazole), 7.57 (dd, 2H, J = 8, 7.4 Hz; Ar-H, H-3 and H-5 of phenyl), 7.67 (d, 2H, J = 7.4 Hz; Ar-H, H-2 and H-6 of phenyl), 7.77 (d, 1H, J = 8 Hz; Ar-H, H-7 of benzothiazole), 7.98 (s, 1H, C=CH̲–ph), 8.01 (d, 1H, J = 7.6 Hz; Ar-H, H-4 of benzothiazole), and 12.87 (s, 1H, NH; D$_2$O exchangeable); Anal. calcd. for C$_{19}$H$_{13}$N$_3$O$_3$S$_2$ (m.w. 395.04): C, 57.71; H, 3.31; N, 10.63; S, 16.21. Found: C, 57.90; H, 3.27; N, 10.53; S, 15.94.

N-(Benzothiazol-2-yl)-2-(5-(2-chlorobenzylidene)-2,4-dioxothiazolidin-3-yl)acetamide (9b)

Yield, 87%; m.p. 195–197°C; IR$_{\nu max}$ (cm^{-1}): 3,197 (NH), 3,065 (CH aromatic), 2,992 (CH aliphatic), and 1,698 (C=O); ^{1}H-NMR (400 MHz, DMSO-d_6): 4.69 (s, 2H, CH$_2$), 7.29 (dd, 1H, J = 7.4, 8 Hz; Ar-H, H-5 of benzothiazol), 7.42 (dd, 1H, J = 7.4, 8.4 Hz; Ar-H, H-6 of benzothiazole), 7.49 (d, 1H, J = 7 Hz; Ar-H, H-6 of phenyl), 7.53 (dd, 1H, J = 7, 7.6 Hz; Ar-H, H-5 of phenyl), 7.62 (d, 1H, J = 8.4 Hz; Ar-H, H-7 of benzothiazole), 7.75 (dd, 1H, J = 7.6, 8 Hz; Ar-H, H-4 of phenyl), 7.90 (s, 1H, C=CH̲–ph), 7.96 (d, 1H, J = 8 Hz; Ar-H, H-4 of benzothiazole), 8.08 (d, 1H, J = 8 Hz; Ar-H, H-3 of phenyl), and 12.85 (s, 1H, NH; D$_2$O exchangeable); MS (m/z): 432 (M$^+$+2, 12.36%), 430 (M$^+$, 27.63%), 429 (100%, base peak), 252 (4.04%), 150 (22.86%), and 56 (15.13%); Anal. calcd. for C$_{19}$H$_{12}$ClN$_3$O$_3$S$_2$ (m.w. 429.89): C, 53.09; H, 2.81; N, 9.77; S, 14.92. Found: C, 53.23; H, 2.74; N, 9.65; S, 14.98.

N-(Benzothiazol-2-yl)-2-(5-(4-chlorobenzylidene)-2,4-dioxothiazolidin-3-yl)acetamide (9c)

Yield, 81%; m.p. 182–184°C; IR$_{\nu max}$ (cm^{-1}): 3,215 (NH), 3,045 (CH aromatic), 2,976 (CH aliphatic), and 1,678 (C=O); ^{1}H-NMR (400 MHz, DMSO-d_6): 4.68 (s, 2H, CH$_2$), 7.28 (dd, 1H, J = 8, 8.4 Hz; Ar-H, H-5 of benzothiazole), 7.41 (dd, 1H, J = 7.6, 8 Hz; Ar-H, H-6 of benzothiazole), 7.60 (d, 2H, J = 8.8 Hz; Ar-H, H-3 and H-5 of phenyl), 7.66 (d, 2H, J = 8.8 Hz; Ar-H, H-2 and H-6 of phenyl), 7.74 (d, 1H, J = 7.6 Hz; Ar-H, H-7 of benzothiazole), 7.96 (d, 1H, J = 8.4 Hz; Ar-H, H-4 of benzothiazole), 7.99 (s, 1H, C=CH̲–ph), and 12.83 (s, 1H, NH; D$_2$O exchangeable); MS (m/z): 431.89 (M$^+$+2, 2.72%), 429.91 (M$^+$, 6.47%), 251.84 (46.03%), 176.86 (100%, base peak), 149.93 (44.78%), and 55.98 (26.90%); Anal. calcd. for C$_{19}$H$_{12}$ClN$_3$O$_3$S$_2$ (m.w. 429.89): C, 53.09; H, 2.81; N, 9.77; S, 14.92. Found: C, 53.32; H, 2.94; N, 9.98; S, 15.04.

N-(Benzothiazol-2-yl)-2-(5-(2,6-dichlorobenzylidene)-2,4-dioxothiazolidin-3-yl)acetamide (9d)

Yield, 80%; m.p. 190–192°C; IR$_{\nu max}$ (cm^{-1}): 3,215 (NH), 3,090 (CH aromatic), 2,935 (CH aliphatic), 1,743, 1,665, 1,659 (2C=O); ^{1}H-NMR (400 MHz, DMSO-d_6): 4.69 (s, 2H, CH$_2$), 7.29 (dd, 1H,

J = 7.6, 7.6 Hz; Ar-H, H-5 of benzothiazole), 7.42 (dd, 1H, J = 7.6, 8 Hz; Ar-H, H-6 of benzothiazole), 7.48 (dd, 1H, J = 8, 8 Hz; Ar-H, H-4 of phenyl), 7.60 (d, 2H, J = 8 Hz; Ar-H, H-3 and H-5 of phenyl), 7.75 (d, 1H, J = 8 Hz; Ar-H, H-7 of benzothiazole), 7.93 (s, 1H, C=CH̲–ph), 7.97 (d, 1H, J = 7.6 Hz; Ar-H, H-4 of benzothiazole), and 12.85 (s, 1H, NH; D$_2$O exchangeable); MS (m/z): 468 (M$^+$+4, 5.11%), 466 (M$^+$+2, 11.69%), 464 (M$^+$, 32.51%), 463 (100%, base peak), 286 (38.23%), 177 (30.88%), and 56 (11.97%); Anal. calcd. for C$_{19}$H$_{11}$Cl$_2$N$_3$O$_3$S$_2$ (m.w. 464.34): C, 49.15; H, 2.39; N, 9.05; S, 13.81. Found: C, 48.75; H, 2.51; N, 9.06; S, 13.54.

N-(Benzothiazol-2-yl)-2-(5-(4-fluorobenzylidene)-2,4-dioxothiazolidin-3-yl)acetamide (9e)

Yield, 85%; m.p. 237–239°C; IR$_{\nu max}$ (cm^{-1}): 3,229 (NH), 3,076 (CH aromatic), 2,984 (CH aliphatic), and 1,679 (C=O); ^{1}H-NMR (400 MHz, DMSO-d_6): 4.68 (s, 2H, CH$_2$), 7.28 (dd, 1H, J = 8, 7.6 Hz; Ar-H, H-5 of benzothiazole), 7.37 (d, 2H, J = 8.4 Hz; Ar-H, H-3 and H-5 of phenyl), 7.42 (dd, 1H, J = 8, 8 Hz; Ar-H, H-6 of benzothiazole), 7.71 (d, 2H, J = 8.4 Hz; Ar-H, H-2 and H-6 of phenyl), 7.74 (d, 1H, J = 8 Hz; Ar-H, H-7 of benzothiazole), 7.96 (d, 1H, J = 7.6 Hz; Ar-H, H-4 of benzothiazole), 8.01 (s, 1H, C=CH̲–ph), and 12.84 (s, 1H, NH; D$_2$O exchangeable); MS (m/z): 415 (M$^+$+2, 14.51%), 413 (M$^+$, 98%), 236 (20.14%), 177 (100%, base peak), 152 (55.65%), and 56 (28.81%); Anal. calcd. for C$_{19}$H$_{12}$FN$_3$O$_3$S$_2$ (m.w. 413.44): C, 55.20; H, 2.93; N, 10.16; S, 15.51. Found: C, 55.34; H, 2.87; N, 9.90; S, 15.52.

N-(Benzothiazol-2-yl)-2-(5-(4-methylbenzylidene)-2,4-dioxothiazolidin-3-yl)acetamide (9f)

Yield, 92%; m.p. 250–252°C; IR$_{\nu max}$ (cm^{-1}): 3,208 (NH), 3,067 (CH aromatic), 2,999 (CH aliphatic), 1,739, 1,698, and 1,659 (3C=O); ^{1}H-NMR (400 MHz, DMSO-d_6): 2.36 (s, 3H, CH$_3$), 4.67 (s, 2H, CH$_2$), 7.29 (dd, 1H, J = 8, 8 Hz; Ar-H, H-5 of benzothiazole), 7.35 (d, 2H, J = 8 Hz; Ar-H, H-3 and H-5 of phenyl), 7.42 (dd, 1H, J = 7.6, 8 Hz; Ar-H, H-6 of benzothiazole), 7.54 (d, 2H, J = 8 Hz; Ar-H, H-2 and H-6 of phenyl), 7.75 (d, 1H, J = 7.6 Hz; Ar-H, H-7 of benzothiazole), 7.95 (s, 1H, C=CH̲–ph), 7.96 (d, 1H, J = 8 Hz; Ar-H, H-4 of benzothiazole), and 12.83 (s, 1H, NH; D$_2$O exchangeable); Anal. calcd. for C$_{20}$H$_{15}$N$_3$O$_3$S$_2$ (m.w. 409.48): C, 58.66; H, 3.69; N, 10.26; S, 15.66. Found: C, 58.37; H, 3.64; N, 10.38; S, 15.83.

N-(Benzothiazol-2-yl)-2-(5-(2-methoxybenzylidene)-2,4-dioxothiazolidin-3-yl)acetamide (9g)

Yield, 80%; m.p. 277–279°C; IR$_{\nu max}$ (cm^{-1}): 3,280 (NH), 3,075 (CH aromatic), 2,940 (CH aliphatic), and 1,681 (C=O); ^{1}H-NMR (400 MHz, DMSO-d_6): 3.89 (s, 3H, OCH$_3$), 4.67 (s, 2H, CH$_2$), 7.09 (dd, 1H, J = 7.6, 8 Hz; Ar-H, H-5 of phenyl), 7.16 (d, 1H, J = 8.4 Hz; Ar-H, H-3 of phenyl), 7.29 (dd, 1H, J = 8.4, 8 Hz; Ar-H, H-4 of phenyl), 7.40 (dd, 1H, J = 8, 8.4 Hz; Ar-H, H-5 of benzothiazole), 7.45 (dd, 1H, J = 7.6, 8.4 Hz; Ar-H, H-6 of benzothiazole), 7.51 (d, 1H, J = 7.6 Hz; Ar-H, H-6 of phenyl), 7.75 (d, 1H, J = 7.6 Hz; Ar-H, H-7 of benzothiazole), 7.96 (d, 1H, J = 8 Hz; Ar-H, H-4 of benzothiazole), 8.11 (s, 1H, C=CH̲–ph), and 12.83 (s, 1H, NH; D$_2$O exchangeable); MS (m/z): 425.89 (M$^+$, 10.31%),

424.90 (38.13%), 247.88 (15.07%), 176.89 (100%, base peak), 120.92 (18.11%), and 76.93 (3.17%); Anal. calcd. for $C_{20}H_{15}ClN_3O_4S_2$ (m.w. 425.48): C, 56.46; H, 3.55; N, 9.88; S, 15.07. Found: C, 56.31; H, 3.68; N, 10.12; S, 15.21.

N-(Benzothiazol-2-yl)-2-(5-(4-methoxybenzylidene)-2,4-dioxothiazo-lidin-3-yl)acetamide (9h)

Yield, 85%; m.p. 270–272°C; $IR_{\nu max}$ (cm^{-1}): 3,210 (NH), 3,059 (CH aromatic), 2,937 (CH aliphatic), 1,683 (C=O), and 1,583 (C=N); ^{1}H-NMR (400 MHz, DMSO-d_6): 3.81 (s, 3H, OCH$_3$), 4.67 (s, 2H, CH$_2$), 7.29 (dd, 1H, J = 7.2, 8 Hz; Ar-H, H-5 of benzothiazole), 7.42 (dd, 1H, J = 7.2, 8.4 Hz; Ar-H, H-6 of benzothiazole), 7.53 (d, 2H, J = 8.8 Hz; Ar-H, H-3 and H-5 of phenyl), 7.61 (d, 2H, J = 8.8 Hz; Ar-H, H-2 and H-6 of phenyl), 7.74 (d, 1H, J = 8.4 Hz; Ar-H, H-7 of benzothiazole), 7.94 (s, 1H, C=CH–ph), 7.96 (d, 1H, J = 8 Hz; Ar-H, H-4 of benzothiazole), and 12.83 (s, 1H, NH; D$_2$O exchangeable); ^{13}C-NMR (100 MHz, DMSO-d_6): δ = 44.01, 55.94, 115.36, 118.01, 120.73, 121.21, 122.29, 124.29, 125.74, 126.72, 132.29 (2C), 132.87 (2C), 134.30, 161.44, 161.83, 165.74, 167.63, and 168.41; Anal. calcd. for $C_{20}H_{15}ClN_3O_4S_2$ (m.w. 425.48): C, 56.46; H, 3.55; N, 9.88; S, 15.07. Found: C, 56.06; H, 3.46; N, 10.43; S, 15.34.

N-(Benzothiazol-2-yl)-2-(5-(4-(dimethylamino)benzylidene)-2,4-diox-othiazolidin-3-yl)acetamide (9i)

Yield, 85%; m.p. 240–242°C; $IR_{\nu max}$ (cm^{-1}): 3,299 (NH), 3,045 (CH aromatic), 2,905 (CH aliphatic), and 1,673 (C=O); ^{1}H-NMR (400 MHz, DMSO-d_6): 3.04 (s, 6H, N(CH$_3$)$_2$), 4.67 (s, 2H, CH$_2$), 6.83 (d, 2H, J = 8.8 Hz; Ar-H, H-3 and H-5 of phenyl), 7.31 (dd, 1H, J = 7.6, 8 Hz; Ar-H, H-5 of benzothiazole), 7.41 (dd, 1H, J = 7.6, 8.4 Hz; Ar-H, H-6 of benzothiazole), 7.49 (d, 2H, J = 8.8 Hz; Ar-H, H-2 and H-6 of phenyl), 7.77 (d, 1H, J = 8.4 Hz; Ar-H, H-7 of benzothiazole), 7.86 (s, 1H, C=CH–ph), 7.99 (d, 1H, J = 8 Hz; Ar-H, H-4 of benzothiazole), and 12.85 (s, 1H, NH; D$_2$O exchangeable); ^{13}C-NMR (100 MHz, DMSO-d_6): δ = 39.34, 43.88, 111.42, 112.50 (2C), 112.57, 113.10, 120.03 (2C), 122.28, 124.27, 126.71, 132.56, 132.97 (2C), 135.28, 152.23 (2C), 165.80, and 167.81; Anal. calcd. for $C_{21}H_{18}N_4O_3S_2$ (m.w. 438.52): C, 57.52; H, 4.14; N, 12.78; S, 14.62. Found: C, 57.27; H, 4.27; N, 12.62; S, 14.27.

N-(Benzothiazol-2-yl)-2-(5-(3-nitrobenzylidene)-2,4-dioxothiazolidin-3-yl)acetamide (9j)

Yield, 89%; m.p. 207–209°C; $IR_{\nu max}$ (cm^{-1}): 3,196 (NH), 3,069 (CH aromatic), 2,988 (CH aliphatic), and 1,694 (C=O); ^{1}H-NMR (400 MHz, DMSO-d_6): 4.70 (s, 2H, CH$_2$), 7.29 (dd, 1H, J = 7.6, 8 Hz; Ar-H, H-5 of benzothiazole), 7.42 (dd, 1H, J = 7.4, 8 Hz; Ar-H, H-6 of benzothiazole), 7.75 (d, 1H, J = 8 Hz; Ar-H, H-6 of phenyl), 7.82 (dd, 1H, J = 8, 8 Hz; Ar-H, H-5 of phenyl), 7.97 (d, 1H, J = 7.4 Hz; Ar-H, H-7 of benzothiazole), 8.06 (d, 1H, J = 8 Hz; Ar-H, H-4 of phenyl), 8.17 (s, 1H, C=CH–ph), 8.31 (d, 1H, J = 7.6 Hz; Ar-H, H-4 of benzothiazole), 8.52 (s, 1H; Ar-H, H-2 of phenyl), and 12.85 (s, 1H, NH; D$_2$O exchangeable); Anal. calcd. for $C_{19}H_{12}N_4O_5S_2$ (m.w. 440.45): C, 51.81; H, 2.75; N, 12.72; S, 14.56. Found: C, 51.99; H, 2.65; N, 12.40; S, 14.61.

4.1.5 | General method for the synthesis of *N*-(benzothiazol-2-yl)-2-((5-cyano-6-oxo-4-(4-(un)-substituted phenyl)-1,6-dihydropyrimidin-2-yl)thio)-acetamide (11a–e)

A mixture of *N*-(benzothiazol-2-yl)-2-chloroacetamide (**7**; 0.23 g, 0.001 mol) and the appropriate 2-mercaptodihydropyrimidine derivatives (**10a–e**; 0.001 mol) in the presence of anhydrous potassium carbonate (0.14 g, 0.001 mol) was refluxed in dry acetone (50 ml) for 8 hr. The reaction mixture was filtered while hot and the residue was washed with hot acetone. The filtrate was concentrated, cooled and poured onto ice water; the precipitated solid product was filtered, washed with water, dried, and recrystallized from ethanol to afford the corresponding target compounds (**11a–e**), respectively.

N-(Benzothiazol-2-yl)-2-((5-cyano-6-oxo-4-phenyl-1,6-dihydropyri-midin-2-yl)thio)acetamide (11a)

Yield, 60%; m.p. 217–219°C; $IR_{\nu max}$ (cm^{-1}): 3,355, 3,186 (2 NH), 3,072 (CH aromatic), 2,980 (CH aliphatic), 2,226 (C≡N), and 1,667 (C=O); ^{1}H-NMR (400 MHz, DMSO-d_6): 4.24 (s, 1H, CH$_2$), 7.19 (dd, 1H, J = 8.8 Hz; Ar-H, H-4 of phenyl), 7.28 (dd, 2H, J = 8, 7.6 Hz; Ar-H, H-3 and H-5 of phenyl), 7.35 (dd, 1H, J = 7.6, 7.4 Hz; Ar-H, H-5 of benzothiazole), 7.42 (dd, 1H, J = 7.6, 10 Hz; Ar-H, H-6 of benzothia-zole), 7.72 (d, 2H, J = 7.6 Hz; Ar-H, H-2 and H-6 of phenyl), 7.74 (d, 1H, J = 10 Hz; Ar-H, H-7 of benzothiazole), 7.95 (d, 1H, J = 7.4 Hz; Ar-H, H-4 of benzothiazole), 12.65 (s, 1H, NHCOCH$_2$; D$_2$O exchange-able), and 13.82 (s, 1H, OH of pyrimidinone; D$_2$O exchangeable); ^{13}C-NMR (100 MHz, DMSO-d_6): δ = 34.90, 92.31, 117.74, 121.03 (2C), 122.19 (2C), 124.05, 126.64, 128.57 (2C), 128.86 (2C), 131.27, 131.92, 136.37, 149.02, 158.27, 167.56, and 167.95; MS (*m/z*): 421 (M$^+$, 8.37%), 339 (54.38%), 313 (100%, base peak), 269 (45.42%), and 69 (18.95%); Anal. calcd. for $C_{20}H_{13}N_5O_2S_2$ (m.w. 419.48): C, 57.27; H, 3.12; N, 16.70; S, 15.29. Found: C, 57.01; H, 3.30; N, 16.60; S, 15.41.

N-(Benzothiazol-2-yl)-2-((5-cyano-4-(4-fluorophenyl)-6-oxo-1,6-di-hydropyrimidin-2-yl)thio)acetamide (11b)

Yield, 70%; m.p. 275–277°C; $IR_{\nu max}$ (cm^{-1}): 3,360, 3,196 (2 NH), 3,068 (CH aromatic), 2,924 (CH aliphatic), 2,220 (C≡N), and 1,666 (C=O); ^{1}H-NMR (400 MHz, DMSO-d_6): 4.28 (s, 1H, CH$_2$), 7.02 (d, 2H, J = 8 Hz; Ar-H, H-3 and H-5 of phenyl), 7.28 (dd, 1H, J = 8, 7.2 Hz; Ar-H, H-5 of benzothiazole), 7.42 (dd, 1H, J = 7.6, 8 Hz; Ar-H, H-6 of benzothiazole), 7.75 (d, 2H, J = 8 Hz; Ar-H, H-2 and H-6 of phenyl), 7.82 (d, 1H, J = 7.6 Hz; Ar-H, H-7 of benzothiazole), 7.94 (d, 1H, J = 7.2 Hz; Ar-H, H-4 of benzothiazole), 12.67 (s, 1H, NHCOCH$_2$; D$_2$O exchangeable), and 13.96 (s, 1H, OH of pyrimidinone; D$_2$O exchangeable); MS (*m/z*): 439 (M$^+$+2, 1.39%), 437 (M$^+$, 4.15%), 329 (59.53%), 287 (100%, base peak), 69 (57.34%), and 45 (26.38%); Anal. calcd. for $C_{20}H_{12}FN_5O_2S_2$ (m.w. 437.47): C, 54.91; H, 2.77; N, 16.01; S, 14.66. Found: C, 54.79; H, 2.88; N, 15.84; S, 14.68.

N-(Benzothiazol-2-yl)-2-((5-cyano-6-oxo-4-(p-tolyl)-1,6-dihydropyrimidin-2-yl)thio)acetamide (11c)

Yield, 55%; m.p. 224–226°C; IR$_{\nu max}$ (cm^{-1}): 3,238, 3,183 (2 NH), 3,053 (CH aromatic), 2,914 (CH aliphatic), 2,221 (C≡N), and 1,664 (C=O); ^{1}H-NMR (400 MHz, DMSO-d_6): 2.13 (s, 3H, CH$_3$), 4.32 (s, 1H, CH$_2$), 6.97 (d, 2H, J = 8 Hz; Ar-H, H-3 and H-5 of phenyl), 7.31 (dd, 1H, J = 7.6, 7.4 Hz; Ar-H, H-5 of benzothiazole), 7.46 (dd, 1H, J = 7.6, 8 Hz; Ar-H, H-6 of benzothiazole), 7.67 (d, 2H, J = 8 Hz; Ar-H, H-2 and H-6 of phenyl), 7.79 (d, 1H, J = 8 Hz; Ar-H, H-7 of benzothiazole), 7.96 (d, 1H, J = 7.4 Hz; Ar-H, H-4 of benzothiazole), 12.69 (s, 1H, NHCOCH$_2$; D$_2$O exchangeable), and 13.91 (s, 1H, OH of pyrimidinone; D$_2$O exchangeable); ^{13}C-NMR (100 MHz, DMSO-d_6): δ = 21.27, 35.02, 93.03, 110.00, 116.40, 120.98, 122.19, 124.09, 126.65, 129.01 (2C), 129.26 (2C), 131.94, 132.63, 142.17, 149.00, 158.27, 165.69, 167.23, and 167.53; Anal. calcd. for C$_{21}$H$_{15}$N$_5$O$_2$S$_2$ (m.w. 433.50): C, 58.18; H, 3.49; N, 16.16; S, 14.79. Found: C, 58.08; H, 3.82; N, 16.01; S, 14.69.

N-(Benzothiazol-2-yl)-2-((5-cyano-4-(4-hydroxyphenyl)-6-oxo-1,6-dihydropyrimidin-2-yl)thio)acetamide (11d)

Yield, 55%; m.p. 209–211°C; IR$_{\nu max}$ (cm^{-1}): 3,432 (OH), 3,190 (NH), 3,050 (CH aromatic), 2,993 (CH aliphatic), 2,248 (C≡N), and 1,660 (C=O); ^{1}H-NMR (400 MHz, DMSO-d_6): 5.15 (s, 1H, CH$_2$), 7.09 (d, 2H, J = 8 Hz; Ar-H, H-3 and H-5 of phenyl), 7.36 (dd, 1H, J = 7.6, 8 Hz; Ar-H, H-5 of benzothiazole), 7.48 (dd, 1H, J = 7.6, 8 Hz; Ar-H, H-6 of benzothiazole), 7.89 (d, 2H, J = 8 Hz; Ar-H, H-2 and H-6 of phenyl), 7.91 (d, 1H, J = 8 Hz; Ar-H, H-7 of benzothiazole), 8.04 (d, 1H, J = 8 Hz; Ar-H, H-4 of benzothiazole), 9.47 (s, 1H, ph–OH; D$_2$O exchangeable), 12.94 (s, 1H, NHCOCH$_2$; D$_2$O exchangeable), and 13.22 (s, 1H, OH of pyrimidinone; D$_2$O exchangeable); Anal. calcd. for C$_{20}$H$_{13}$N$_5$O$_3$S$_2$ (m.w. 435.48): C, 55.16; H, 3.01; N, 16.08; S, 14.72. Found: C, 55.20; H, 3.31; N, 15.80; S, 14.82.

N-(Benzothiazol-2-yl)-2-((5-cyano-4-(4-methoxyphenyl)-6-oxo-1,6-dihydropyrimidin-2-yl)thio)acetamide (11e)

Yield, 65%; m.p. 244–246°C; IR$_{\nu max}$ (cm^{-1}): 3,344, 3,205 (2 NH), 3,075 (CH aromatic), 2,991 (CH aliphatic), 2,233 (C≡N), and 1,663 (C=O); ^{1}H-NMR (400 MHz, DMSO-d_6): 3.57 (s, 3H, OCH$_3$), 4.27 (s, 1H, CH$_2$), 6.67 (d, 2H, J = 7.6 Hz; Ar-H, H-3 and H-5 of phenyl), 7.28 (dd, 1H, J = 7.6, 7.6 Hz; Ar-H, H-5 of benzothiazole), 7.42 (dd, 1H, J = 7.6, 8.4 Hz; Ar-H, H-6 of benzothiazole), 7.76 (d, 2H, J = 7.6 Hz; Ar-H, H-2 and H-6 of phenyl), 7.78 (d, 1H, J = 8.4 Hz; Ar-H, H-7 of benzothiazole), 7.95 (d, 1H, J = 7.6 Hz; Ar-H, H-4 of benzothiazole), 12.69 (s, 1H, NHCOCH$_2$; D$_2$O exchangeable), and 13.77 (s, 1H, OH of pyrimidinone; D$_2$O exchangeable); Anal. calcd. for C$_{21}$H$_{15}$N$_5$O$_3$S$_2$ (m.w. 449.50): C, 56.11; H, 3.36; N, 15.58; S, 14.26. Found: C, 56.03; H, 3.62; N, 15.65; S, 14.46.

4.2 | Docking studies

In the present work, all the target compounds were subjected to docking study to explore their binding mode towards VEGFR-2 enzyme. All modeling experiments were performed using Molsoft program which provides a unique set of tools for the modeling of protein–ligand interactions. It predicts how small flexible molecule such as substrates or drug candidates bind to a protein of known three-dimensional structure represented by grid interaction potentials (http://www.molsoft.com/icm_pro.html). Each experiment used the biological target VEGFR-2 downloaded from the Brookhaven Protein Databank (http://www.rcsb.org/pdb/explore/explore.do?structureId=1YWN). To qualify the docking results in terms of accuracy of the predicted binding conformations in comparison with the experimental procedure, the reported VEGFR-2 inhibitor drugs vatalanib and sorafenib were used as reference ligands.

4.3 | In vitro cytotoxic activity

The cytotoxicity assays were performed at the Pharmacology and Toxicology Department, Faculty of Pharmacy, Al-Azhar University, Cairo, Egypt. Cancer cells from different cancer cell lines HepG2, MCF-7, and HCT-116, were purchased from American Type Cell Culture Collection (ATCC; Manassas) and grown on the appropriate growth medium Roswell Park Memorial Institute medium (RPMI 1640) supplemented with 100 mg/ml of streptomycin, 100 units/ml of penicillin, and 10% of heat-inactivated fetal bovine serum in a humidified, 5% (v/v) CO$_2$ atmosphere at 37°C. Cytotoxicity assay was performed by using MTT.

The exponentially growing cells from different cancer cell lines were trypsinized, counted, and seeded at the appropriate densities (2,000–1,000 cells/0.33 cm^2 well) into 96-well microtiter plates. Cells then were incubated in a humidified atmosphere at 37°C for 24 hr. Then, cells were exposed to different concentrations of compounds (0.1, 10, 100, and 1,000 µM) for 72 hr. Then the viability of treated cells was determined using MTT technique as follow. Media were removed; cells were incubated with 200 µl of 5% MTT solution/well (Sigma-Aldrich, MO) and were allowed to metabolize the dye into colored-insoluble formazan crystals for 2 hr. The remaining MTT solution was discarded from the wells and the formazan crystals were dissolved in a 200-µl/well acidified isopropanol for 30 min, covered with aluminum foil and with continuous shaking using a MaxQ 2000 plate shaker (Thermo Fisher Scientific Inc, MI) at room temperature. Absorbance was measured at 570 nm using a Stat FaxR 4200 plate reader (Awareness Technology, Inc., FL). The cell viability was expressed as a percentage of control and the concentration that induces 50% of maximum inhibition of cell proliferation (IC$_{50}$) was determined using GraphPad Prism version 5 software (GraphPad Software Inc., CA).[43–45]

4.4 | In vitro VEGFR-2 kinase assay

The kinase activity of VEGFR-2 was carried out in the Pharmacology and Toxicology Department, Faculty of Pharmacy, Al-Azhar University, Cairo, Egypt, and measured by use of an antiphosphotyrosine antibody with the Alpha Screen system (PerkinElmer) according to manufacturer's instructions.[15] Enzyme reactions were performed in 50 mM Tris-HCl pH 7.5, 5 mM MnCl$_2$, 5 mM MgCl$_2$, 0.01% Tween-20 and 2 mM dithiothreitol,

containing 10 μM ATP, 0.1 μg/ml biotinylated poly-GluTyr (4:1) and 0.1 nM of VEGFR-2 (Millipore, UK). Before the catalytic initiation with ATP, the tested compounds at final concentrations ranging from 0 to 300 μg/ml and enzyme were incubated for 5 min at room temperature. The reactions were quenched by the addition of 25 μl of 100 mM ethylenediaminetetraacetic acid, 10 μg/ml Alpha Screen streptavidin donor beads, and 10 μg/ml acceptor beads in 62.5 mM 4-(2-hydroxyethyl)-1-piperazineethanesulfonic acid pH 7.4, 250 mM NaCl, and 0.1% bovine serum albumin. The plate was incubated in the dark overnight and then read by ELISA Reader (PerkinElmer). Wells containing the substrate and the enzyme without compounds were used as reaction control. Wells containing biotinylated poly-GluTyr (4:1) and enzyme without ATP were used as basal control. Percent inhibition was calculated by the comparison of compounds treated to control incubations. The concentration of the test compound causing 50% inhibition (IC_{50}) was calculated from the concentration–inhibition response curve (triplicate determinations) and the data were compared with sorafenib (Sigma-Aldrich) as standard VEGFR-2 inhibitor.

ACKNOWLEDGMENTS

CONFLICT OF INTERESTS

The authors declare that there are no conflicts of interests.

ORCID

Ibrahim H. Eissa http://orcid.org/0000-0002-6955-2263
Khaled El-Adl http://orcid.org/0000-0002-8922-9770

REFERENCES

[1] E. Oksuzoglu, B. Tekiner-Gulbas, S. Alper, O. Temiz-Arpaci, T. Ertan, I. Yildiz, N. Diril, E. Sener-Aki, I. Yalcin, J. Enzyme Inhib. Med. Chem. 2008, 23, 37. https://doi.org/10.1080/14756360701342516

[2] D. Kumar, M. B. Reynolds, S. M. Kerwin, Bioorg. Med. Chem. 2002, 10, 3997. https://doi.org/10.1016/S0968-0896(02)00327-9

[3] S. Kakkar, S. Tahlan, S. M. Lim, K. Ramasamy, V. Mani, S. A. A. Shah, B. Narasimhan, Chem. Cent. J. 2018, 12, 92. https://doi.org/10.1186/s13065-018-0459-5

[4] M. H. Potashman, J. Bready, A. Coxon, T. M. DeMelfi, L. DiPietro, N. Doerr, D. Elbaum, J. Estrada, P. Gallant, J. Germain, Y. Gu, J.-C. Harmange, S. A. Kaufman, R. Kendall, J. L. Kim, G. N. Kumar, A. M. Long, S. Neervannan, V. F. Patel, A. Polverino, P. Rose, S. van der Plas, D. Whittington, R. Zanon, H. Zhao, J. Med. Chem. 2007, 50, 4351. https://doi.org/10.1021/jm070034i

[5] M. A. Abdelgawad, A. Belalb, O. M. Ahmed, J. Chem. Pharm. Res. 2013, 5, 318.

[6] S. Sulthana, P. Pandian, J. Drug Deliv. Ther. 2019, 9, 505. https://doi.org/10.22270/jddt.v9i1-s.2358

[7] D. Osmaniye, S. Levent, A. B. Karaduman, S. Ilgın, Y. Özkay, Z. A. Kaplancıklı, Molecules 2018, 23, 1054. https://doi.org/10.3390/molecules23051054

[8] E. A. Abd El-Meguid, Int. J. Pharm. Technol. 2015, 7, 10040.

[9] Y. Oguro, D. R. Cary, N. Miyamoto, M. Tawada, H. Iwata, H. Miki, A. Hori, S. Imamura, Bioorg. Med. Chem. 2013, 21, 4714.

[10] G. Niu, X. Chen, Curr. Drug Targets 2010, 11, 1000.

[11] K. Holmes, O. L. Roberts, A. M. Thomas, M. J. Cross, Cell. Signal. 2007, 19, 2003.

[12] S. Tugues, S. Koch, L. Gualandi, X. Li, L. Claesson-Welsh, Mol. Aspects Med. 2011, 32, 88.

[13] W. M. Eldehna, H. S. Ibrahim, H. A. Abdel-Aziz, N. N. Farrag, M. M. Youssef, Eur. J. Med. Chem. 2015, 89, 549.

[14] W. M. Eldehna, S. M. Abou-Seri, A. M. El Kerdawy, R. R. Ayyad, H. A. Ghabbour, M. M. Ali, D. A. Abou El Ella, Eur. J. Med. Chem. 2016, 113, 50. https://doi.org/10.1016/j.ejmech.2016.02.029

[15] S. M. Abou-Seri, W. M. Eldehna, M. M. Ali, D. A. Abou El Ella, Eur. J. Med. Chem. 2016, 107, 165. https://doi.org/10.1016/j.ejmech.2015.10.053

[16] P. Wu, T. E. Nielsen, M. H. Clausen, Trends Pharmacol. Sci. 2015, 36, 422.

[17] S. Wilhelm, C. Carter, M. Lynch, T. Lowinger, J. Dumas, R. A. Smith, B. Schwartz, R. Simantov, S. Kelley, Nat. Rev. Drug Discov. 2006, 5, 835.

[18] A. Pircher, W. Hilbe, I. Heidegger, J. Drevs, A. Tichelli, M. Medinger, Int. J. Mol. Sci. 2011, 12, 7077. https://doi.org/10.3390/ijms12107077

[19] Q.-Q. Xie, H.-Z. Xie, J.-X. Ren, L.-L. Li, S.-Y. Yang, J. Mol. Graph. Model. 2009, 27, 751.

[20] K. Lee, K.-W. Jeong, Y. Lee, J. Y. Song, M. S. Kim, G. S. Lee, Y. Kim, Eur. J. Med. Chem. 2010, 45, 542.

[21] R. N. Eskander, K. S. Tewari, Gynecol. Oncol. 2014, 132, 496.

[22] V. A. Machado, D. Peixoto, R. Costa, H. J. Froufe, R. C. Calhelha, R. M. Abreu, I. C. Ferreira, R. Soares, M.-J. R. Queiroz, Bioorg. Med. Chem. 2015, 23, 6497.

[23] J. Dietrich, C. Hulme, L. H. Hurley, Bioorg. Med. Chem. 2010, 18, 5738.

[24] A. Garofalo, L. Goossens, P. Six, A. Lemoine, S. Ravez, A. Farce, P. Depreux, Bioorg. Med. Chem. Lett. 2011, 21, 2106.

[25] M. A. Aziz, R. A. Serya, D. S. Lasheen, A. K. Abdel-Aziz, A. Esmat, A. M. Mansour, A. N. B. Singab, K. A. Abouzid, Sci. Rep. 2016, 6, 1–20. https://doi.org/10.1038/srep24460

[26] L. Zhang, Y. Shan, X. Ji, M. Zhu, C. Li, Y. Sun, R. Si, X. Pan, J. Wang, W. Ma, B. Dai, B. Wang, J. Zhang, Oncotarget 2017, 8, 104745. https://doi.org/10.18632/oncotarget.20065

[27] H. M. Patel, P. Bari, R. Karpoormath, M. Noolvi, N. Thapliyal, S. Surana, P. Jain, RSC Adv. 2015, 5, 56724.

[28] S. R. Pattan, P. kekare, N. S. Dighe, S. A. Nirmal, D. S. Musmade, S. K. Parjane, A. V. Daithankar, J. Chem. Pharm. Res. 2009, 1, 191.

[29] P. Sharma, T. S. Reddy, D. Thummuri, K. R. Senwar, N. P. Kumar, V. Naidu, S. K. Bhargava, N. Shankaraiah, Eur. J. Med. Chem. 2016, 124, 608.

[30] A. T. Taher, S. M. Abou-Seri, Molecules 2012, 17, 9868.

[31] C. Viegas-Junior, A. Danuello, V. da Silva Bolzani, E. J. Barreiro, C. A. M. Fraga, Curr. Med. Chem. 2007, 14, 1829.

[32] A. A. El-Helby, R. R. A. Ayyad, H. Sakr, K. El-Adl, M. M. Ali, F. Khedr, Arch. Pharm. Chem. Life Sci. 2017, 350, e1700240. https://doi.org/10.1002/ardp.201700240

[33] A. A. El-Helby, H. Sakr, R. R. A. Ayyad, K. El-Adl, M. M. Ali, F. Khedr, Med. Chem. 2018, 18, 1. https://doi.org/10.2174/1871520618666180412123833

[34] Q.-Q. Xie, H.-Z. Xie, J.-X. Ren, L.-L. Li, S.-Y. Yang, J. Mol. Graph. Model. 2009, 27, 751.

[35] K. Lee, K.-W. Jeong, Y. Lee, J. Y. Song, M. S. Kim, G. S. Lee, Y. Kim, *Eur. J. Med. Chem.* **2010**, *45*, 542.

[36] M. M. Raj, H. V. Patel, L. M. Raj, N. K. Patel, *Int. J. Pharm. Chem. Biol. Sci.* **2013**, *3*, 814.

[37] S. R. Pattan, P. kekare, N. S. Dighe, S. A. Nirmal, D. S. Musmade, S. K. Parjane, A. V. Daithankar, *J. Chem. Pharm. Res.* **2009**, *1*, 191.

[38] S. A. H. El-Feky, H. A. Abd El-Fattah, N. A. Osman, M. Imran, M. N. Zedan, *J. Chem. Pharm. Res.* **2015**, *7*, 1154.

[39] B. Baum, M. Mohamed, M. Zayed, C. Gerlach, A. Heine, D. Hangauer, G. Klebe, *J. Mol. Biol.* **2009**, *390*, 56.

[40] L. Englert, A. Biela, M. Zayed, A. Heine, D. Hangauer, G. Klebe, *Biochim. Biophys. Acta* **2010**, *1800*, 1192.

[41] A. A. El-Helby, R. R. A. Ayyad, K. El-Adl, H. Sakr, A. A. Abd-Elrahman, I. H. Eissa, A. Elwan, *Med. Chem. Res.* **2016**, *25*, 3030.

[42] A. A. El-Helby, R. R. A. Ayyad, K. El-Adl, A. Elwan, *Med. Chem. Res.* **2017**, *26*, 2967.

[43] T. Mosmann, *J. Immunol. Methods* **1983**, *65*, 55.

[44] D. A. Scudiero, R. H. Shoemaker, K. D. Paull, A. Monks, S. Tierney, T. H. Nofziger, M. J. Currens, D. Seniff, M. R. Boyd, *Cancer Res.* **1988**, *48*, 4827.

[45] F. M. Freimoser, C. A. Jakob, M. Aebi, U. Tuor, *Appl. Environ. Microbiol.* **1999**, *65*, 3727.

SUPPORTING INFORMATION

Additional supporting information may be found online in the Supporting Information section.